
DECORRELATIVE NETWORK ARCHITECTURE FOR ROBUST ELECTROCARDIOGRAM CLASSIFICATION

A PREPRINT

Christopher Wiedeman

Department of Electrical and Computer Systems Engineering
Rensselaer Polytechnic Institute
Troy, NY, 12180, USA
wiedec@rpi.edu

Ge Wang*

Department of Biomedical Engineering
Rensselaer Polytechnic Institute
Troy, NY, 12180, USA
wang6@rpi.edu

July 20, 2022

ABSTRACT

Artificial intelligence has made great progresses in medical data analysis, but the lack of robustness and interpretability has kept these methods from being widely deployed. In particular, data-driven models are vulnerable to adversarial attacks, which are small, targeted perturbations that dramatically degrade model performance. As a recent example, while deep learning has shown impressive performance in electrocardiogram (ECG) classification, Han et al. crafted realistic perturbations that fooled the network 74% of the time Han et al. [2020]. Current adversarial defense paradigms are computationally intensive and impractical for many high dimensional problems. Previous research indicates that a network vulnerability is related to the features learned during training. We propose a novel approach based on ensemble decorrelation and Fourier partitioning for training parallel network arms into a decorrelated architecture to learn complementary features, significantly reducing the chance of a perturbation fooling all arms of the deep learning model. We test our approach in ECG classification, demonstrating a much-improved 77.2% chance of at least one correct network arm on the strongest adversarial attack tested, in contrast to a 21.7% chance from a comparable ensemble. Our approach does not require expensive optimization with adversarial samples, and thus can be scaled to large problems. These methods can easily be applied to other tasks for improved network robustness.

Keywords Deep Learning, Electrocardiogram, Adversarial Attack Stability, Ensemble Learning

1 Introduction

The exponential increase in high-dimensional patient datasets and constant demand for personalized healthcare justify the urgent need for artificial intelligence (AI) in medicine. For example, electrocardiograms (ECG), previously reserved to in-patient observation, are potentially available in smart or implantable devices. Such technology has the capacity to improve preventative healthcare by continuously monitoring for signs of heart diseases, even alerting medical services to emergency situations before they occur. While big data can be leveraged in this situation, it is infeasible to have human clinicians analyze these signals in real-time, making AI a natural solution to this problem Ebrahimi et al. [2020], Murat et al. [2020], Xiao et al. [2022], Hong et al. [2020].

To this end, many researchers have applied deep learning to ECG classification. The 2017 PhysioNet Challenge is a milestone in this field, where deep neural networks (DNNs) were trained to classify atrial fibrillation from single-lead ECG signals Clifford et al. [2017]. The top-scoring models can often achieve high classification accuracies on test data, but their interpretability and robustness are a major concern Goodfellow et al. [2018]. Chief among these concerns is the existence of adversarial attacks, which have been demonstrated both in machine learning broadly and healthcare

*Correspondence: wang6@rpi.edu

tasks specifically. As misdiagnosis can cause serious harm, recognizing conditions where a system cannot perform well is crucial Elul et al. [2021].

1.1 Adversarial Attacks: Background and Characteristics

First publicized in 2014, adversarial attacks to an input are small perturbations that do not change the semantic content as perceived by a human yet cause massive errors in a network output Szegedy et al. [2014]. A common example would be imperceptible noise patterns added to an image, which causes a model to misclassify the image. Mathematically, this is formulated by maximizing the loss objective J of the model f by modifying x (with the paired label y) within a set of valid perturbations Δ :

$$\begin{aligned} & \underset{\delta}{\text{maximize}} && J(x + \delta, y) \\ & \text{subject to} && \delta \in \Delta(x) \end{aligned} \tag{1}$$

The most studied perturbation set is an ℓ_∞ -norm bounded ball, since it is assumed that samples within a small ball share the same semantic content, but the set of meaning-invariant perturbations is domain specific. The most commonly used method for solving this optimization for ℓ_∞ bound attacks is an iterative, first-order algorithm called projected gradient descent (PGD) Madry et al. [2019], Ren et al. [2020]. Various other approaches exist, including the use of generative adversarial ensembles Song et al. [2018], Xiao et al. [2019], Liu and Hsieh [2019]. Impressively, *universal adversarial perturbations* can be crafted to fool a network when added to any sample Moosavi-Dezfooli et al. [2016], Chaubey et al. [2020].

The understanding of adversarial attacks in deep learning has been rapidly developed over the past few years. Akhtar and Mian wrote a broad survey on adversarial attacks in computer vision Akhtar and Mian [2018]. Initially, adversarial instability was conflated with overfitting of a complex, non-linear model. However, it was quickly distinguished as a separate phenomenon, since these DNNs often generalize well to unseen data yet fail on previously seen data that are only slightly altered Goodfellow et al. [2015]. Furthermore, it was shown that linear models and other machine learning methods are also vulnerable to adversarial attacks Papernot et al. [2016a]. Subsequently, much research focused on the lack of data in high-dimensional problems leaving a large part of the total ‘data-manifold’ unstable Gilmer et al. [2018], Dube [2018]. Literature also reported a relationship between large local Lipschitz constants (with regards to the loss function) and adversarial instability Qin et al. [2019], Hein and Andriushchenko [2017], Roth et al. [2020-10-23]. To our knowledge, the most unifying, coherent explanation is the robust features model, where it is shown (in a classification setting) that data distributions often exhibit statistical patterns that are semantically meaningless to humans but correlated well with different classes Ilyas et al. [2019]. From a human’s perspective, these patterns are arbitrary and easily perturbed, but since models are only incentivized to maximize distributional accuracy, they have no reason to prioritize the features humans associate with relevant objects over these patterns.

Training models for defending against adversarial attacks remains an open problem, affecting nearly every application of machine learning. Early attempts at defense methods by *obfuscating* the loss gradient were found to beat only weak attackers, proving ineffective for sophisticated attackers Athalye et al. [2018], Carlini and Wagner [2017], Uesato et al. [2018], Carlini and Wagner [2016], Papernot et al. [2016b]. To date, adversarial training, in which a model is iteratively trained on strong adversarial samples, has shown the best results in terms of adversarial robustness Madry et al. [2019], Kurakin et al. [2017]. However, the network size and computational time required is considerable for small problems and entirely infeasible otherwise.

Another troubling, well-documented characteristic of these attacks is their *transferability*: models trained on the same task will often be fooled by the same attacks, despite having different parameters Szegedy et al. [2014], Papernot et al. [2016a], Tramèr et al. [2017]. This phenomenon is largely congruent with the robust features model, since these models are likely learning the same useful, but non-robust features. Nevertheless, transferability makes black-box attacks viable, where a malicious attacker does not necessarily have access to the detailed knowledge of a model.

1.2 Key Ideas: Ensemble Decorrelation and Fourier Partitioning

Our primary goal is to find practical solutions for training a DNN with improved adversarial stability without compromising the overall performance. We use ECG classification as a proxy task, since Han, et al. recently showed that models trained for this attack are susceptible to natural-looking adversarial attacks Han et al. [2020]. In short, these researchers observed that traditional ℓ_∞ PGD attacks produce square-wave artifacts that are not physiologically plausible in ECG signals; as such, they modified the perturbation space by applying smoothing kernels in the attack objective, rendering plausible yet still highly effective adversarial samples. As a high-dimensional problem, it is not

feasible to adversarially train models for robust ECG classification. In contrast, we seek to instead train multiple classification network arms with diverse weaknesses and integrate them together via ensemble learning to achieve an accurate and stable performance.

The motivation behind our adversarial ensemble learning approach is to add stability via redundancy, assuming that the other networks will succeed where one fails. Unfortunately, simply training networks with different parameters does not achieve this due to the aforementioned transferability of the attacks between different models. According to the robust features model, this means that when trained in isolation, different networks still tend to converge toward the same learned features and vulnerabilities. Therefore, *a mechanism for incentivizing networks to learn different features is necessary*. To this end, Yang, et al. conceived DVERGE, which is a method to diversify the learned features and adversarial weaknesses in a classification ensemble Yang et al. [2020]. However, this method still requires at least the partial computation of adversarial samples and round-robin style training of networks, which is expensive and impractical for larger problems.

Consequently, we propose two distinct methods for diversifying learned features, and test these against adversarial ECG attacks in Han et al. [2020]. The first method, linear feature decorrelation, is based on our earlier work Wiedeman and Wang [2022], which not only found a strong linear correlation between in the latent space of networks trained on the same task, but also found that adding a loss term to reduce the linear correlation greatly decreases the transferability of adversarial attacks. However, the decorrelation process proposed in that work is rather expensive, as it requires large batch sizes and parallel training of networks. Here we first seek to accelerate this decorrelation process greatly. The second method is heuristically simpler, employing linear time-invariant filters to partition the input space by frequency, forcing networks to learn features in different frequency bands. This method is inspired by recently discovered connections between the Fourier space and adversarial stability, which not only demonstrated that neural networks can make accurate inferences by relying only on low or high-frequency characteristics but also that most robustifying training methods only shift a network’s sensitivity to different frequency bands Yin et al. [2019]. As such, we find that a crude but efficient way to teach different networks different features is to partition the original inputs by frequency, feeding data in different bands to different networks and integrate their outputs via ensemble learning.

2 Results

We trained four different ensembles for ECG classification. Each ensemble consists of three models. The first is initialized as the trained model used to test ECG adversarial attacks in Han et al. [2020]. The other two are separately trained auxiliary models with the identical architecture Goodfellow et al. [2018].

The first ensemble (**cor**) acts as a control, where both auxiliary models were trained traditional (i.e., cross entropy minimization) with no mechanism for diversifying the models. In the decorrelated ensemble, (**dec**), a feature decorrelation objective was added when training the auxiliary models. The exact methodology of the decorrelation was substantially modified from Wiedeman and Wang [2022] to make the computation feasible for larger problems. In short, decorrelation was performed at the final regression feature layer, which was further compressed via random projection, and only one model was actively trained at one time (Figure 1; see details in the Materials and Methods section). The Fourier partitioned ensemble (**fcor**) used only the traditional cross entropy objective, but inputs to either auxiliary model were pre-filtered by the complementary filters (Figure 2) for both training and inference. The final ensemble (**fdec**) combines the decorrelation and Fourier partitioning methods into a unified ensemble.

Ensembles produce multiple inferences, which can in turn be processed in a variety of ways to aggregate a single answer or gauge uncertainty. Consequently, for natural samples and adversarial samples of varying magnitude, we define the following evaluation metrics:

- Average: the average classification accuracy over all models.
- P(‘x’ model): probability of at least ‘x’ (of three) model(s) correctly classifying a sample, where $x=1,2,3$.

Figure 3 compares these results for PGD attacks of varying strength. Additionally, Figure 4 displays this same analysis for physiologically feasible, smoothed adversarial perturbations (SAP) Han et al. [2020], while Figure 5 evaluates this for natural test samples.

3 Discussions

The first surprising result is a relatively low transferability of small magnitude attacks was found in our investigation. The study in Han et al. [2020] only investigated $\varepsilon = 10$ perturbations and reported that their smooth attacks were still fooled the network 74% of the time. Despite this success rate, Figure 4 shows nearly an 80% chance that at

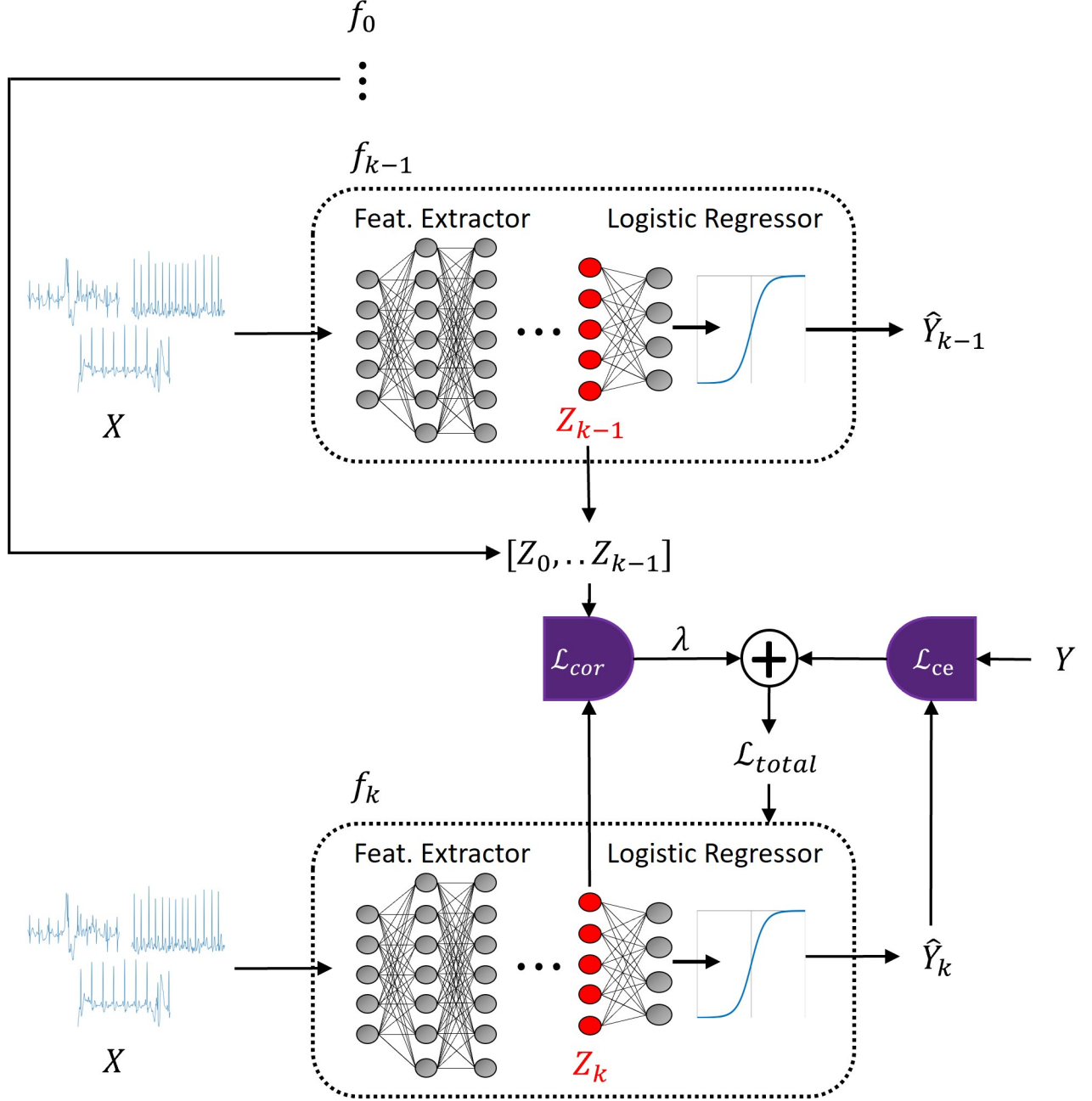


Figure 1: Illustration of the decorrelation training process. The current model f_k is trained using both cross entropy and a correlation loss. The correlation loss references previous models' extracted sample features as opposed to training multiple models in parallel.

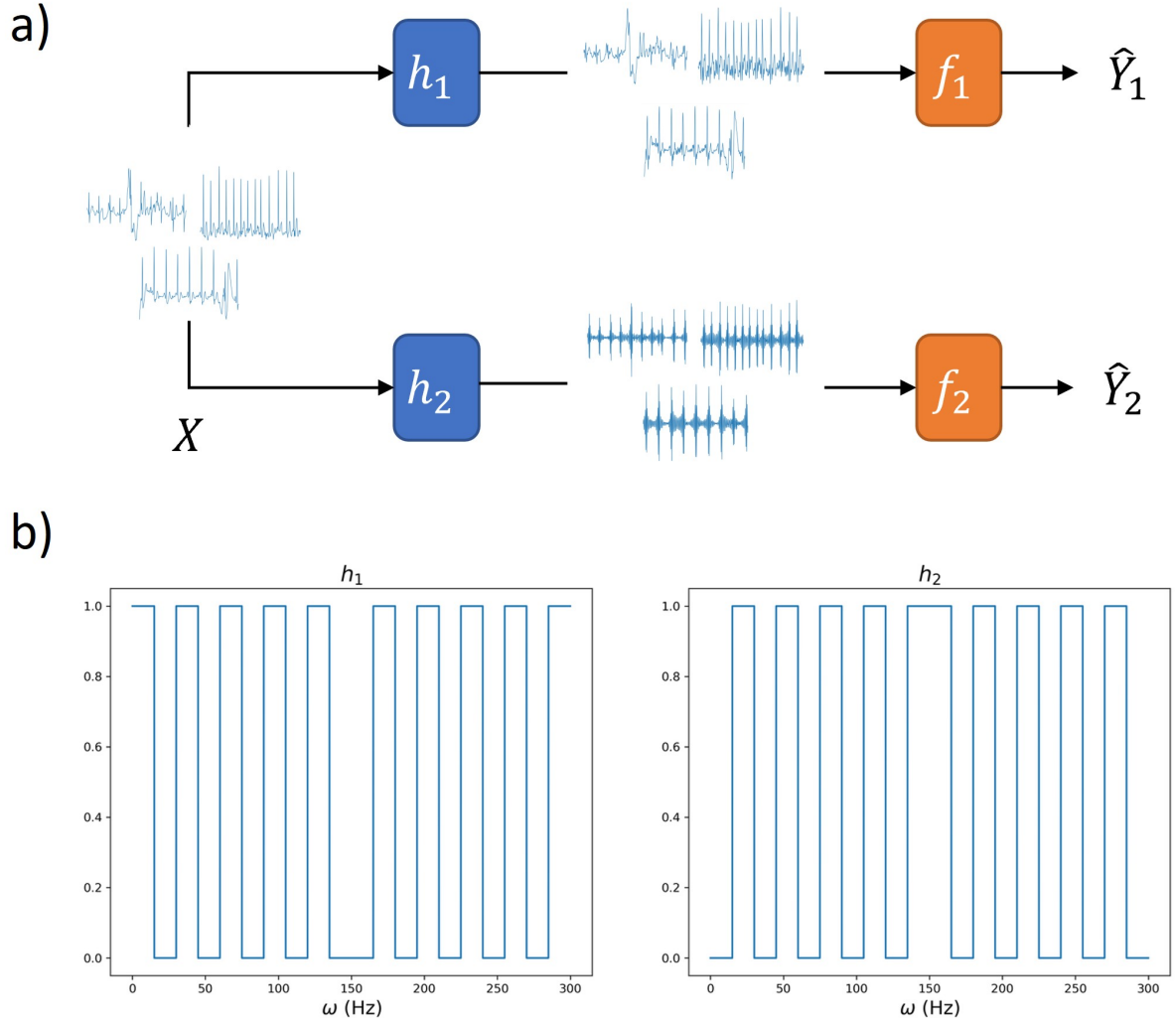


Figure 2: Illustration of Fourier transform-based input data decomposition. a) Diagram showing frequency partitioning each sample into two inputs, which are fed into different models, where h is a partitioning filter, and f is a classification model; and b) the frequency responses of h_1 and h_2 (real-valued only).

least two models in the cor ensemble will correctly classify the attacked samples, and >90% chance that at least one model will do classification correctly under the attacks. Figure 3 gives a similar story for traditional PGD attacks. This lack of immediate transferability could be due to the large size of the network, whose complexity might help reduce the adversarial transferability Madry et al. [2019]. However, this initial robustness plummets in the face of more challenging, larger magnitude attacks, as seen in Figures 3 and 4.

dec, fdec, and fcor, all achieved higher average, $P(1 \text{ correct})$, and $P(2 \text{ correct})$ scores against PGD and SAP attacks at $\varepsilon = 10$ as compared to what cor did. More importantly, the decline in these metrics as attack strength increases is not nearly as severe, which indicates much better robustness under these conditions. For example, for $\varepsilon = 150$ smoothed adversarial perturbations, there is only a 21% chance that at least one model in the cor ensemble correctly classifies the sample (indicating poor ensemble diversity), as opposed to a 77% chance the fdec ensemble has. This gap shows distinct potential for the training methods in creating diverse ensembles.

While both dec and fcor outperformed cor in the adversarial ensemble setting, fdec generally produces the best results (Figures 3 and 4), implying that the Fourier partitioning and decorrelation methods are synergistic, and can be easily combined for even better robustness. To investigate this further, we saved the features extracted from the training set using each model and calculated the overall linear correlation coefficient between each feature set. The different ensembles and relationships between models via correlation coefficients are illustrated in Figure 6. The coefficients

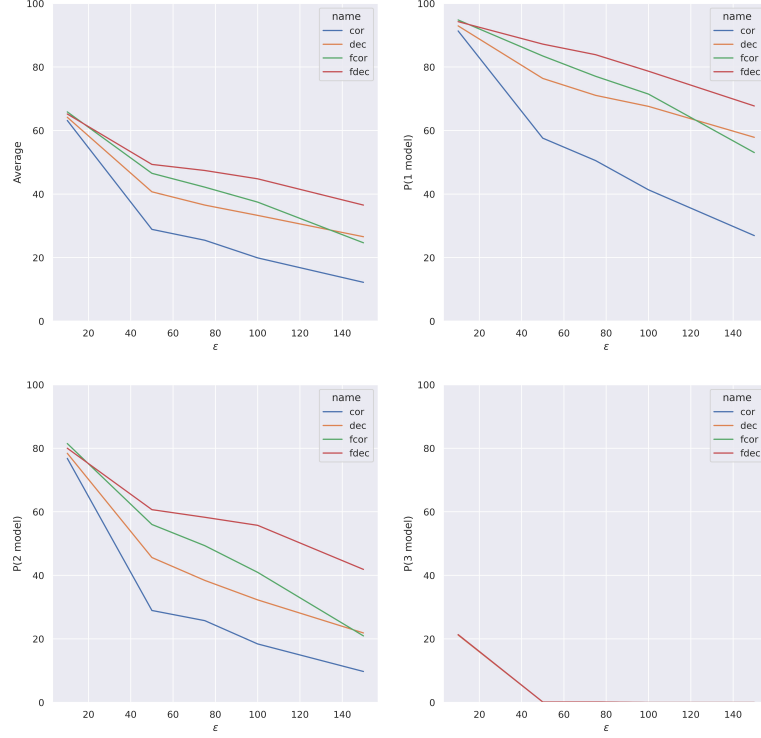


Figure 3: Ensemble classification performance on PGD adversarial attacks with varying strength ϵ , as measured by average ensemble accuracy (top left), probability of at least one correct prediction (top right), probability of at least two correct predictions (bottom left) and all correct predictions (bottom right) on the adversarial samples.

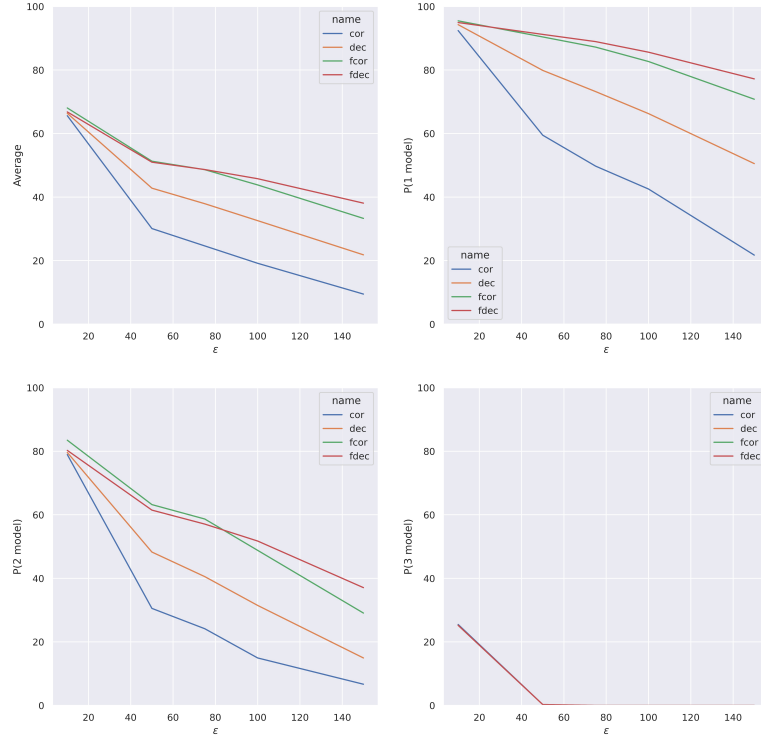


Figure 4: Ensemble classification performance on smoothed adversarial perturbations of varying strength ϵ , as measured by average ensemble accuracy (top left), probability of at least one correct prediction (top right), probability of at least two correct predictions (bottom left) and all correct predictions (bottom right) on the adversarial samples.

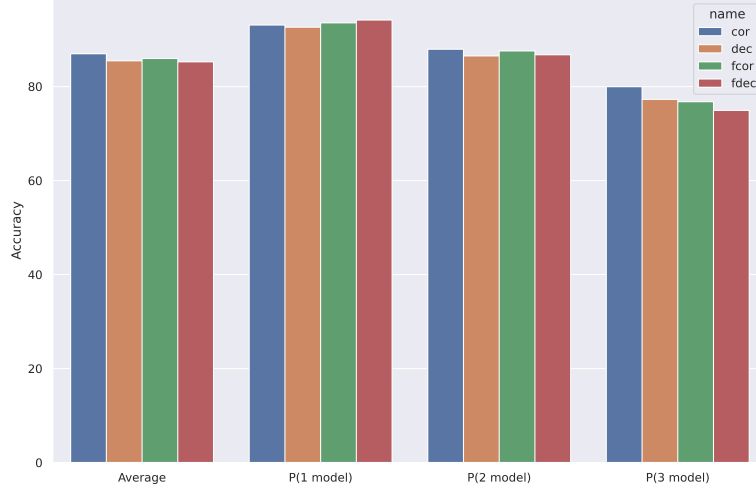


Figure 5: Ensemble classification performance on natural test samples, as measured by average ensemble accuracy, probability of at least one correct prediction (top right), probability of at least two correct predictions, and all correct predictions.

between models in dec and fdec are clearly lower than the coefficients in cor, which is due to the decorrelation mechanism during training. fcor, however, still has correlation coefficients comparable to cor, suggesting that Fourier partitioning is not simply a proxy for decorrelation, but rather a distinct mechanism for increasing robustness altogether. As such, it is not surprising that implementing both methods produces the best results.

The most exciting aspect of this work is the ease of implementation and scalability of both the proposed decorrelation mechanism and the Fourier partitioning scheme. Using the fast Fourier transform, Fourier partitioning is a simple and efficient way to force models to rely on different features. In theory, the filters should be designed such that the output of any single filter does not hold all the original information, but some combination of all filter outputs preserves all the original information. Our experiments simply used two ‘ring filters’ which summed to an impulse response, but many other schemes could be explored in the same spirit.

Previous work Wiedeman and Wang [2022] mentioned several challenges with scaling decorrelated ensembles to larger problems: 1) the original scheme trained models in parallel, which scales the memory with the ensemble size, 2) the regression requires the batch size to exceed the dimension of the selected feature space such that the linear system is overdetermined; and 3) singular value decomposition is done for each feature batch, which can be expensive for large matrices. With regards to the first problem, we found that instead of training and decorrelating multiple models simultaneously, holding previously trained models fixed and then simply decorrelating the current model in training is still effective. By leveraging this new scheme, only the batch features from previous models need to be loaded in addition to the current model and training batch, greatly reducing the memory demand. In regards to the second two challenges, we must reduce the dimension of the feature space. In most classification networks, the final hidden feature layer represents the highest level, most distilled representation. We found that selecting this layer for decorrelation did not interfere with the classification accuracy and is much more efficient for decorrelation since it is much more compressed than previous layers. The feature space is further compressed using random projections (i.e., one set of features was randomly projected into a lower dimensional space). Since this projection is random with each training step, the optimizer cannot ‘cheat’ by only decorrelating features in a subspace; thus the entire feature space is still decorrelated over the entire training cycle.

It can be seen in Figure 5 that the average natural accuracies for dec, fcor, and fdec are slightly below the natural accuracy of cor. This could indicate an inherent tradeoff between feature diversification and classification accuracy. That is, there is likely a set of features which best maximize distributional accuracy over a dataset, and all networks will converge towards these features when only trying to minimize cross entropy only. In the case of decorrelation training, networks must compromise between learning useful features and learning features dissimilar from those learned by previous networks. In the Fourier partitioning scheme, each network can only extract features from part of the sample bandwidth.

In this work, we have studied ensemble diversification in the context of adversarial attacks, but the ideas presented can apply to other areas of robustness, such as common image corruptions, out-of-sample detection, etc. In many healthcare related tasks where AI can work alongside clinicians, and incorrect diagnoses can cause harm, predicting

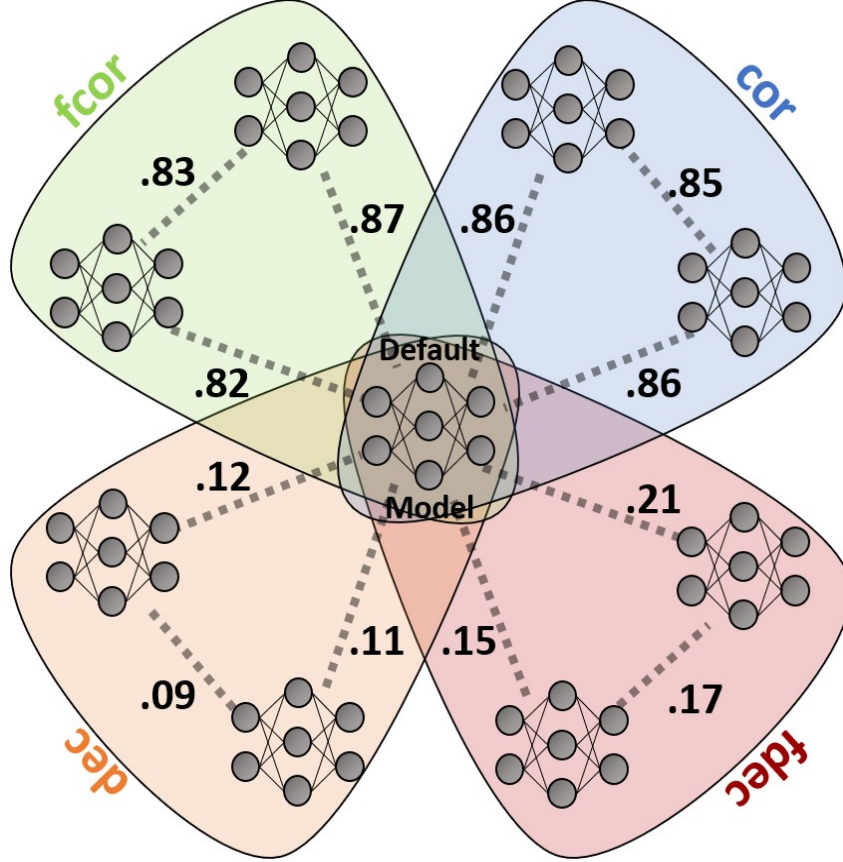


Figure 6: Illustrations of the different models and their informational relationships. Colored areas designate different ensembles, each of which contain three models. Numbers connecting two models represents the overall linear correlation coefficient of the features extracted between the two models over the training data.

model confidence on samples is crucial. One method for estimating model uncertainty is to sample the parameter space by training an ensemble and comparing each model’s output to measure the outcome confidence Wilson and Izmailov [2020], Wilson [2020]. We see applications of this approach for robust uncertainty estimation with a diversified ensemble, which discourages different models from extracting redundant features.

4 Conclusion

In summary, we have presented a novel approach for a decorrelative network architecture (DNA) using two unique training methods: a streamlined and accelerated decorrelation training strategy and a Fourier partitioning scheme. We have applied this approach to ensemble learning for ECG classification and tested them for transferability against state-of-the-art adversarial ECG attacks, demonstrating their merits and great potential in solving large problems. We speculate various future applications, such as tomographic image reconstruction, radiomics, and confidence prediction.

5 Materials and Methods

5.1 Ensemble Training

Each ensemble consisted of three classification networks, each with the architecture in [5]. The first model in every ensemble was loaded as the pre-trained model from Han et al. [2020], which we refer to as the ‘base model’. The other two ‘auxiliary models’ were then trained using the various methods previously described. Each network was trained for 200 epochs (batch size of 80) using the Adam optimizer with a learning rate of 10^{-3} . Pytorch 1.8.1 was used with two NVIDIA Titan RTX GPUs. All other data preprocessing and augmentation procedures were identical to those used in Han et al. [2020] (90/10 training/test split).

5.2 Adversarial Attacks

Two algorithms were used to craft adversarial attacks: projected gradient descent (PGD) and smoothed adversarial perturbations (SAP). PGD is widely used as a strong attack with an ℓ_∞ bound through the following iterative optimization Madry et al. [2019]:

$$x'_i = \text{Clip}_\varepsilon(x'_{i-1} + \alpha \text{sgn}(\nabla_x L(f(x'_{i-1}), y))) \quad (2)$$

where x'_i is the sample at the i^{th} iteration, y is the corresponding label, α is a step size, L is the loss function, and the clipping operation clips all values to be within the ℓ_∞ ball of radius ε around x , as well as any implicit bounds on the domain of X .

SAP is a variation of PGD designed to craft smooth attacks for ECG signals. The details of SAP can be found in Han et al. [2020], but in short, iterative optimization is done over a new variable θ , which is convolved with a sequence of M Gaussian kernels, each of which are parameterized by their width s and standard deviation σ :

$$\begin{aligned} \theta_i &= \text{Clip}_\varepsilon(\theta'_{i-1} + \alpha \text{sgn}(\nabla_\theta L(f(x'(\theta_{i-1})), y))) \\ x'(\theta) &= x + \frac{1}{M} \sum_{m=1}^M \theta \otimes K(s_m, \sigma_m) \end{aligned} \quad (3)$$

The convolution with Gaussian kernels smooths high frequency perturbations, removing unrealistic square wave artifacts. PGD and SAP attacks were optimized over 20 steps in total. For both attacks, α was scaled as $\varepsilon/10$. All adversarial attacks were crafted to target the (pre-loaded) base model, as it was included in all the ensembles. Additionally, adversarial samples were only counted in the results if the base model had classified the corresponding natural sample correctly.

5.3 Decorrelation training

The idea and implementation of the earlier version of our decorrelation training scheme is explained in Wiedeman and Wang [2022]. In short, the intent of decorrelation is to reduce the correlation coefficient between the features extracted from two networks in a latent space. If $Z_1, Z_2 \in \mathbb{R}^{N \times D}$ are the extracted features from batch X with models f_1 and f_2 respectively (N is the batch size, D is the latent dimension), then the Pearson correlation coefficient is found using ordinary least squares to regress a relationship between Z_1 and Z_2 :

$$\begin{aligned} R^2 &= 1 - \frac{SS_{res}}{SS_{total}} = 1 - \frac{\|(I - (\mathbf{Z}_1^\top \mathbf{Z}_1)^{-1} \mathbf{Z}_1^\top) \mathbf{Z}_2\|_2^2}{\|\mathbf{Z}_2\|_2^2} \\ \text{where } \mathbf{Z}_1 &= [Z_1, 1] \end{aligned} \quad (4)$$

To reduce this term during training, the decorrelation loss is defined as:

$$\begin{aligned} \mathcal{L}_R &= \log(SS_{total} + \epsilon) - \log(SS_{res} + \epsilon) \\ \mathcal{L}_R(Z_1, Z_2) &= \log(\|\mathbf{Z}_2\|_2^2 + \epsilon) - \log(\|(I - (\mathbf{Z}_1^\top \mathbf{Z}_1)^{-1} \mathbf{Z}_1^\top) \mathbf{Z}_2\|_2^2 + \epsilon) \end{aligned}$$

where ϵ is some small constant for stability (set to 10^{-5} in our experiments). Due to the pseudo-inverse computation, which requires $N > D$ and singular value decomposition as well as the parallel model training paradigm. Hence, this mechanism cannot scale to larger problems. To solve the above problem, we make the following improvements.

First, we choose the feature layer just prior to the final logistic regression for decorrelation. In most classifiers, this point represents the highest-level features, and is typically much smaller in dimension (size 64 in our networks) than that of the other layers.

Second, we compress the regressor variable using a random projection into a space of dimension $r = 50$. Since a random projection is drawn with each training batch, it is not possible for the algorithm to only decorrelate a subspace

of the original feature space. Additionally, with each training batch we randomly specify which extracted feature batch acts as the regressor and which as the regressand, our new loss is expressed as follows:

$$\mathcal{L}_R^* = \begin{cases} \mathcal{L}_R(Z_1, RZ_2) & \text{with prob. } 0.5 \\ \mathcal{L}_R(Z_2, RZ_1) & \text{with prob. } 0.5 \end{cases}$$

$$R \in R^{D \times r} \sim N(0, 1/\sqrt{D})$$

Finally, we remove the need for training multiple networks in parallel by training networks sequentially and holding the features of previously trained models constant. After training a model, its extracted features on all training samples are saved. While training the next model, these features are loaded with the corresponding batch samples, and then used for decorrelation. As such rather than dynamically decorrelating multiple networks at once, which requires simultaneous training of all networks, we simply use the features extracted by the previously trained networks as constant values to decorrelate against. For decorrelating against multiple models, we average the modified correlation loss against all the previously trained models. Thus, the entire decorrelation loss for model k in an ensemble:

$$\mathcal{L}_{cor}(Z_k, Z_{k-1} \cdots Z_0) = \frac{1}{k-1} \sum_{i=0}^{k-1} \mathcal{L}_R^*(Z_k, Z_i) \quad (5)$$

Figure 1 illustrates the sequential training of the decorrelated ensemble. The total loss for model k is

$$\mathcal{L}_{total} = \mathcal{L}_{ce}(f_k(x), y) + \lambda \mathcal{L}_{cor}(Z_k, Z_{k-1} \cdots Z_0) \quad (6)$$

where y denotes the label, z_j is the feature vector extracted from x by model j , and λ , a hyperparameter set to 0.2 in our experiments.

5.4 Fourier Partitioning Scheme

With the Fourier partitioning scheme, the models were trained normally but inputs were filtered during both training and inference (Figure 2). In practice, filter convolution was done by pointwise multiplication in the Fourier domain, computed using the fast Fourier transform.

6 Data Code and Availability

Data used in this paper is from the 2017 PhysioNet Cardiology Challenge Clifford et al. [2017]. Code for replicating implementing and replicating experiments will be released upon acceptance of this paper for publication.

7 Acknowledgments

This work was partially supported by U.S. National Institute of Health (NIH) grants R01EB026646, R01CA233888, R01CA237267, R01HL151561, R21CA264772, and R01EB031102.

References

- Xintian Han, Yuxuan Hu, Luca Foschini, Larry Chinitz, Lior Jankelson, and Rajesh Ranganath. Deep learning models for electrocardiograms are susceptible to adversarial attack. *Nature Medicine*, 26(3):360–363, 2020.
- Zahra Ebrahimi, Mohammad Loni, Masoud Daneshdatab, and Arash Gharehbaghi. A review on deep learning methods for ECG arrhythmia classification. *Expert Systems with Applications: X*, 7:100033, 2020. ISSN 2590-1885. doi:10.1016/j.eswax.2020.100033. URL <https://www.sciencedirect.com/science/article/pii/S2590188520300123>.
- Fatma Murat, Ozal Yildirim, Muhammed Talo, Ulas Baran Baloglu, Yakup Demir, and U. Rajendra Acharya. Application of deep learning techniques for heartbeats detection using ECG signals-analysis and review. *Computers in Biology and Medicine*, 120:103726, 2020. ISSN 0010-4825. doi:10.1016/j.compbiomed.2020.103726. URL <https://www.sciencedirect.com/science/article/pii/S0010482520301104>.

- Jianbiao Xiao, Jiahao Liu, Huanqi Yang, Qingsong Liu, Ning Wang, Zhen Zhu, Yulong Chen, Yu Long, Liang Chang, Liang Zhou, and Jun Zhou. Ulecnet: An ultra-lightweight end-to-end ecg classification neural network. *IEEE Journal of Biomedical and Health Informatics*, 26(1):206–217, 2022. doi:10.1109/JBHI.2021.3090421.
- Shenda Hong, Zhou Yuxi, Junyuan Shang, Cao Xiao, and Sun Jimeng. Opportunities and challenges of deep learning methods for electrocardiogram data: A systematic review. *Computers in Biology and Medicine*, 122, 2020.
- Gari Clifford, Chengyu Liu, Benjamin Moody, Li-wei Lehman, Ikaro Silva, Qiao Li, Alistair Johnson, and Roger Mark. Af classification from a short single lead ECG recording: the physionet computing in cardiology challenge 2017, 2017. URL <http://www.cinc.org/archives/2017/pdf/065-469.pdf>.
- Sebastian D. Goodfellow, Andrew Goodwin, Robert Greer, Peter C. Laussen, Mjaye Mazwi, and Danny Eytan. Towards understanding ECG rhythm classification using convolutional neural networks and attention mappings. In *Proceedings of the 3rd Machine Learning for Healthcare Conference*, pages 83–101. PMLR, 2018. URL <https://proceedings.mlr.press/v85/goodfellow18a.html>. ISSN: 2640-3498.
- Yonatan Elul, Aviv A. Rosenberg, Assaf Schuster, Alex M. Bronstein, and Yael Yaniv. Meeting the unmet needs of clinicians from ai systems showcased for cardiology with deep-learning-based ecg analysis. *Proceedings of the National Academy of Sciences*, 118(24):e2020620118, 2021. doi:10.1073/pnas.2020620118. URL <https://www.pnas.org/doi/abs/10.1073/pnas.2020620118>.
- Christian Szegedy, Wojciech Zaremba, Ilya Sutskever, Joan Bruna, Dumitru Erhan, Ian Goodfellow, and Rob Fergus. Intriguing properties of neural networks, 2014. URL <http://arxiv.org/abs/1312.6199>.
- Aleksander Madry, Aleksandar Makelov, Ludwig Schmidt, Dimitris Tsipras, and Adrian Vladu. Towards deep learning models resistant to adversarial attacks. *arXiv:1706.06083 [cs, stat]*, 2019. URL <http://arxiv.org/abs/1706.06083>.
- Kui Ren, Tianhang Zheng, Zhan Qin, and Xue Liu. Adversarial attacks and defenses in deep learning. *Engineering*, 6(3):346–360, 2020. ISSN 2095-8099. doi:10.1016/j.eng.2019.12.012. URL <https://www.sciencedirect.com/science/article/pii/S209580991930503X>.
- Yang Song, Rui Shu, Nate Kushman, and Stefano Ermon. Constructing unrestricted adversarial examples with generative models. *arXiv:1805.07894 [cs, stat]*, 2018. URL <http://arxiv.org/abs/1805.07894>.
- Chaowei Xiao, Bo Li, Jun-Yan Zhu, Warren He, Mingyan Liu, and Dawn Song. Generating adversarial examples with adversarial networks. *arXiv:1801.02610 [cs, stat]*, 2019. URL <http://arxiv.org/abs/1801.02610>.
- Xuanqing Liu and Cho-Jui Hsieh. Rob-GAN: Generator, discriminator, and adversarial attacker. *arXiv:1807.10454 [cs, stat]*, 2019. URL <http://arxiv.org/abs/1807.10454>.
- Seyed-Mohsen Moosavi-Dezfooli, Alhussein Fawzi, and Pascal Frossard. DeepFool: a simple and accurate method to fool deep neural networks. *arXiv:1511.04599 [cs]*, 2016. URL <http://arxiv.org/abs/1511.04599>.
- Ashutosh Chaubey, Nikhil Agrawal, Kavya Barnwal, Keerat K. Guliani, and Pramod Mehta. Universal adversarial perturbations: A survey. *arXiv:2005.08087 [cs]*, 2020. URL <http://arxiv.org/abs/2005.08087>.
- Naveed Akhtar and Ajmal Mian. Threat of adversarial attacks on deep learning in computer vision: A survey. *IEEE Access*, 6:14410–14430, 2018. ISSN 2169-3536. doi:10.1109/ACCESS.2018.2807385. Conference Name: IEEE Access.
- Ian J. Goodfellow, Jonathon Shlens, and Christian Szegedy. Explaining and harnessing adversarial examples. *arXiv:1412.6572 [cs, stat]*, 2015. URL <http://arxiv.org/abs/1412.6572>.
- Nicolas Papernot, Patrick McDaniel, and Ian Goodfellow. Transferability in machine learning: from phenomena to black-box attacks using adversarial samples. *arXiv:1605.07277 [cs]*, 2016a. URL <http://arxiv.org/abs/1605.07277>.
- Justin Gilmer, Luke Metz, Fartash Faghri, Samuel S. Schoenholz, Maithra Raghu, Martin Wattenberg, and Ian Goodfellow. Adversarial spheres. *arXiv:1801.02774 [cs]*, 2018. URL <http://arxiv.org/abs/1801.02774>.
- Simant Dube. High dimensional spaces, deep learning and adversarial examples. *arXiv:1801.00634 [cs]*, 2018. URL <http://arxiv.org/abs/1801.00634>.
- Chongli Qin, James Martens, Sven Gowal, Dilip Krishnan, Krishnamurthy Dvijotham, Alhussein Fawzi, Soham De, Robert Stanforth, and Pushmeet Kohli. Adversarial robustness through local linearization. *arXiv:1907.02610 [cs, stat]*, 2019. URL <http://arxiv.org/abs/1907.02610>.
- Matthias Hein and Maksym Andriushchenko. Formal guarantees on the robustness of a classifier against adversarial manipulation. *Advances in Neural Information Processing Systems*, 30, 2017.
- Kevin Roth, Yannic Kilcher, and Thomas Hofmann. Adversarial training is a form of data-dependent operator norm regularization. *arXiv:1906.01527 [cs, stat]*, 2020-10-23. URL <http://arxiv.org/abs/1906.01527>.

- Andrew Ilyas, Shibani Santurkar, Dimitris Tsipras, Logan Engstrom, Brandon Tran, and Aleksander Madry. Adversarial examples are not bugs, they are features. *arXiv:1905.02175 [cs, stat]*, 2019. URL <http://arxiv.org/abs/1905.02175>.
- Anish Athalye, Nicholas Carlini, and David Wagner. Obfuscated gradients give a false sense of security: Circumventing defenses to adversarial examples. *arXiv:1802.00420 [cs]*, 2018. URL <http://arxiv.org/abs/1802.00420>.
- Nicholas Carlini and David Wagner. Adversarial examples are not easily detected: Bypassing ten detection methods. *arXiv:1705.07263 [cs]*, 2017. URL <http://arxiv.org/abs/1705.07263>.
- Jonathan Uesato, Brendan O’Donoghue, Aaron van den Oord, and Pushmeet Kohli. Adversarial risk and the dangers of evaluating against weak attacks. *arXiv:1802.05666 [cs, stat]*, 2018. URL <http://arxiv.org/abs/1802.05666>.
- Nicholas Carlini and David Wagner. Defensive distillation is not robust to adversarial examples. *arXiv:1607.04311 [cs]*, 2016. URL <http://arxiv.org/abs/1607.04311>.
- Nicolas Papernot, Patrick McDaniel, Xi Wu, Somesh Jha, and Ananthram Swami. Distillation as a defense to adversarial perturbations against deep neural networks. *arxiv*, 2016b.
- Alexey Kurakin, Ian Goodfellow, and Samy Bengio. Adversarial examples in the physical world. *arXiv:1607.02533 [cs, stat]*, 2017. URL <http://arxiv.org/abs/1607.02533>.
- Florian Tramèr, Nicolas Papernot, Ian Goodfellow, Dan Boneh, and Patrick McDaniel. The space of transferable adversarial examples. *arXiv:1704.03453 [cs, stat]*, 2017. URL <http://arxiv.org/abs/1704.03453>.
- Huanrui Yang, Jingyang Zhang, Hongliang Dong, Nathan Inkawhich, Andrew Gardner, Andrew Touchet, Wesley Wilkes, Heath Berry, and Hai Li. DVERGE: Diversifying vulnerabilities for enhanced robust generation of ensembles. *arXiv:2009.14720 [cs, stat]*, 2020. URL <http://arxiv.org/abs/2009.14720>.
- Christopher Wiedeman and Ge Wang. Disrupting adversarial transferability in deep neural networks. *Patterns*, page 100472, 2022. ISSN 26663899.
- Dong Yin, Raphael Gontijo Lopes, Jon Shlens, Ekin Dogus Cubuk, and Justin Gilmer. A fourier perspective on model robustness in computer vision. In H. Wallach, H. Larochelle, A. Beygelzimer, F. d’ Alché-Buc, E. Fox, and R. Garnett, editors, *Advances in Neural Information Processing Systems*, volume 32. Curran Associates, Inc., 2019. URL <https://proceedings.neurips.cc/paper/2019/file/b05b57f6add810d3b7490866d74c0053-Paper.pdf>.
- Andrew G Wilson and Pavel Izmailov. Bayesian deep learning and a probabilistic perspective of generalization. In *Advances in Neural Information Processing Systems*, volume 33, pages 4697–4708. Curran Associates, Inc., 2020. URL <https://proceedings.neurips.cc/paper/2020/hash/322f62469c5e3c7dc3e58f5a4d1ea399-Abstract.html>.
- Andrew Gordon Wilson. The case for bayesian deep learning, 2020. URL <http://arxiv.org/abs/2001.10995>. Number: arXiv:2001.10995.